Nicergoline inhibits human platelet Ca^{2+} signalling through triggering a microtubule-dependent reorganisation of the platelet ultrastructure.

T Walford, F I Musa & A G S Harper

Institute for Science and Technology in Medicine – Keele University, Guy Hilton Research Centre, Thornburrow Drive, Hartshill, United Kingdom, ST4 7QB. United Kingdom.

Running Title - Nicergoline inhibits platelet Ca^{2+} signalling

Corresponding Author. Dr Alan G.S. Harper. Institute for Science and Technology in Medicine – Keele University, Guy Hilton Research Centre, Thornburrow Drive, Hartshill, United Kingdom, ST4 7QB. United Kingdom. a.g.s.harper@keele.ac.uk +44 (0)1782-674472.

Author contribution statement - Experiments were designed by A.G.S. Harper. T. Walford, F.I. Musa and A.G.S. Harper collected and analysed the data. The manuscript was written by T. Walford, F.I. Musa and A.G.S. Harper. All authors participated in manuscript revision and have given final approval for publication.

Word count

Abstract: 245 words

Main: 6064 words

This article has been accepted for publication and undergone full peer review but has not been through the copyediting, typesetting, pagination and proofreading process, which may lead to differences between this version and the Version of Record. Please cite this article as doi: 10.1111/bph.13361

Abstract

Background and Purpose: Recently we have demonstrated that a pericellular Ca^{2+} recycling system potentiates agonist-evoked Ca^{2+} signalling and granule secretion in human platelets, and hypothesised a role for the membrane complex (MC) in orchestrating the accumulation of Ca^{2+} in the pericellular region. Previous work has demonstrated that treatment with high concentrations of nicergoline may disrupt the MC through an ability to trigger a reorganisation of the dense tubular system. Experiments were therefore performed to assess whether nicergoline-induced changes in platelet ultrastructure affects thrombin-evoked Ca^{2+} fluxes and dense granule secretion. **Experimental Approach:** Thrombin-evoked Ca^{2+} fluxes were monitored in Fura-2- or Fluo-5N-loaded human platelets, or using platelet suspensions containing Fluo-4 or Rhod-5N K^+ salts. Fluorescence microscopy was utilised to monitor microtubule structure and intracellular Ca^{2+} store distribution in TubulinTracker- and Fluo-5N-loaded platelets respectively. Dense granule secretion was monitored using luciferin-luciferase. **Key Results:** Nicergoline treatment inhibited thrombin-evoked Ca^{2+} signalling, and induced alterations in the microtubule structure and the distribution of intracellular Ca^{2+} stores in platelets. Nicergoline altered the generation and spreading of thrombin-induced pericellular Ca^{2+} signals and almost completely prevented dense granule secretion. Stabilisation of microtubules using taxol reversed most effects of nicergoline on platelet Ca^{2+} signalling and partially reversed its effects on dense granule secretion. **Conclusions and Implications:** Nicergoline-induced alterations to platelet ultrastructure disrupts platelet Ca^{2+} signalling in a manner that would be predicted if the MC had been disrupted. These data suggest that nicergoline may be a useful prototype for the discovery of novel MC-disrupting anti-thrombotics.

Abbreviations

BSA - Bovine Serum Albumin
$[Ca^{2+}]_{cyt}$ - Cytosolic Ca^{2+} concentration
$[Ca^{2+}]_{ext}$ - Extracellular Ca^{2+} concentration
$[Ca^{2+}]_{st}$ - Intracellular store Ca^{2+} concentration
$[Ca^{2+}]_{peri}$ - Pericellular Ca^{2+} concentration
CICR - Ca^{2+}-induced Ca^{2+} release
CMB – Cortical Microtubule Bundle
DMSO - Dimethyl Sulfoxide
DTS - Dense Tubular System
EGTA – Ethylene Glycol Tetraacetic Acid
HBS – HEPES –buffered saline
MC - Membrane Complex
NCX - Na^{+}/Ca^{2+} exchanger
OCS - Open Canalicular System
PBS – Phosphate-buffered Saline
PMCA – Plasma Membrane Ca^{2+}-ATPase
PRP – Platelet-rich Plasma
STIM1 – Stromal Interaction molecule 1
Thr – Thrombin

Introduction

Upon damage to the vasculature, a variety of agonists trigger the activation and aggregation of human platelets via a rise in the cytosolic Ca^{2+} concentration ($[Ca^{2+}]_{cyt}$; Rink and Sage, 1990). Rises in $[Ca^{2+}]_{cyt}$ activate a variety of different processes required for thrombus formation and thus understanding the mechanisms by which platelets generate and shape their Ca^{2+} signals may allow us to identify novel targets for anti-thrombotics drugs (Heemskerk *et al*., 2013). Recently we have observed that agonist-evoked Ca^{2+} removal in platelets does not appear to occur across the surface membrane but instead occurs into the narrow tunnels of the open canalicular system (OCS; a series of plasma membrane invaginations which spread through the platelets; van Nispen tot Pannerden, 2010; White, 1972;). This creates a pericellular Ca^{2+} accumulation which is able to act as an additional Ca^{2+} source to help maintain agonist-evoked Ca^{2+} signals by recycling back into the platelet cytosol through Ca^{2+}-permeable channels (Sage *et al*., 2013). Experimental manipulations which prevented or buffered this pericellular Ca^{2+} rise were found to inhibit agonist-evoked rises in $[Ca^{2+}]_{cyt}$, dense granule secretion and platelet aggregation – suggesting that this pericellular Ca^{2+} recycling is essential for efficient agonist-evoked activation of human platelets (Sage *et al*., 2013).

Fluorescence imaging showed that the pericellular Ca^{2+} rises were not homogenously distributed throughout the OCS but were found to be generated at specific subcellular regions of the platelets leading to highly-localised Ca^{2+} accumulations of around 50 nm in diameter (which were designated *hotspot*; Sage *et al*., 2013). These observations indicate that platelet calcium removal mechanisms must be specifically localised to a specialised cellular microdomain. This possibility is further predicted by our demonstration that the rate of Ca^{2+} removal from platelets on the low-affinity Na^{+}/Ca^{2+} exchanger (NCX) is near-maximal, even though the peak $[Ca^{2+}]_{cyt}$ in the bulk cytosol (0.4 μM) is found to be significantly below that required for half-maximal activity of this exchanger (0.6-6 μM) (Blaustein and Lederer, 1999; Sage *et al*., 2013) – suggesting that the NCX must be exposed to a microdomain of heightened $[Ca^{2+}]_{cyt}$. Previous work in smooth muscle cells has demonstrated that nanojunctions made up of the tight apposition of the sarcoplasmic reticulum and plasma membrane provides highly-efficient, rapid Ca^{2+} transport between the SR and extracellular environment (van Breemen *et al*, 2013). Platelets possess an analogous nanojunction called the membrane complex (MC), which is formed by the close apposition of the OCS and Dense Tubular System (DTS; the platelet equivalent of the endoplasmic reticulum; van Nispen tot Pannerden, 2010; White, 1972). This lead us to hypothesise that the MC is the point of creation of the Ca^{2+} hotspots we observed in the pericellular region of the cell, and that disruption of the structural integrity of the MC could form a novel mechanism of action for anti-thrombotic drugs. This possibility is supported by previous reports of human bleeding disorders associated with disruption of the MC (Canizares *et al*., 1990; Green *et al*., 1981; Meiamed *et al*., 1984; Parker *et al*., 1993). Intriguingly one patient with a disrupted MC structure was found to have a defect in thrombin-evoked Ca^{2+} signalling (Parker *et al*., 1993) – in line with our predictions for a role of this structure in coordinating agonist-evoked rises in $[Ca^{2+}]_{cyt}$.

Examining the role of the MC in platelets is currently difficult due to the limited amount of information regarding how this cellular architecture may be formed and held together. A literature search was therefore conducted to examine whether there was any previous evidence for an experimental manipulation that could disrupt the MC. From this search, we identified a previous report that high concentrations of the α-adrenoreceptor blocker, nicergoline, can trigger a reorganisation of both the OCS and DTS through a disruption to the

cortical microtubule bundle (Le Menn *et al*., 1979). The link between microtubule reorganisation and DTS redistribution was particularly interesting as the initial report of the MC mentioned that microtubules could occasionally be seen to lie in the junctional space of the MC (White, 1972). We therefore hypothesised that nicergoline might exert its inhibitory effects on platelet function through microtubule-dependent disruption of the MC.

The nicergoline-induced ultrastructural disruption appears to be a secondary effect of this drug as it occurs at a much higher concentration ($IC_{50} \approx 10^{-5}$ M) than required to block adrenoreceptor signalling ($IC_{50} \approx 10^{-7}$ M; Lanza *et al.*, 1986; Le Menn *et al*., 1979). The clear discrepancy in concentrations required to elicit these two effects of nicergoline on platelets provides an opportunity to experimentally distinguish between these different actions of this drug. Interestingly, nicergoline at the higher concentrations required for ultrastructural reorganisation is effective in inhibiting agonist-induced platelet adhesion, aggregation and granule secretion (Lanza *et al.*, 1986; Le Menn *et al*., 1979). Experiments were therefore performed to examine whether nicergoline-induced ultrastructural disruption affects agonist-evoked Ca^{2+} signalling in a manner consistent with an effect on the MC (Parker *et al*., 1993; Sage *et al*, 2013).

Materials and Methods

Materials

FFP-18 K^+ salt (also known as Fura-2 NM K^+ salt) and Fura-2/AM were from TEFlabs Inc. (Austin, TX). Thrombin was from Merck Chemicals (Nottingham, U.K.). TubulinTracker, Fluo-5N/AM and K^+ salts of Rhod-5N and Fluo-4 were from Invitrogen (Paisley, U.K.). Taxol was obtained from Cambridge Biosciences (Cambridge, U.K.). Gö6976 and Alexa Fluor®488-labelled anti-KDEL antibody were from Abcam (Cambridge, U.K.). Nicergoline was obtained from Tocris Bioscience (Bristol, U.K.). Apyrase and luciferin–luciferase were from Sigma Aldrich (Gillingham, U.K.). Ibidi µ slide 8 well chambered coverslips were purchased from Thistle Scientific (Glasgow, U.K.) All other reagents were of analytical grade.

Platelet preparation

This study was approved by the Keele University Research Ethics Committee. Blood was donated by healthy, drug-free volunteers who gave written informed consent. Blood was collected by venepuncture and mixed with one-sixth volume of acid citrate dextrose anticoagulant (85 $mmol.L^{-1}$ sodium citrate, 78 $mmol.L^{-1}$ citric acid, and 111 $mmol.L^{-1}$ D-glucose) and platelet-rich plasma (PRP) prepared by centrifugation for 5 min at 700 *g*, before aspirin (100 $\mu mol.L^{-1}$) and apyrase (0.1 $U.mL^{-1}$) were added.

Monitoring thrombin-evoked Ca^{2+} fluxes

Thrombin-evoked changes in $[Ca^{2+}]_{cyt}$, $[Ca^{2+}]_{peri}$ and intracellular store Ca^{2+} concentration ($[Ca^{2+}]_{st}$) were monitored in Fura-2-, FFP-18- and Fluo-5N-loaded platelets respectively using our previously published methodologies (See Figure 1; Sage *et al*., 2011; Sage *et al*., 2013). Changes in divalent cation permeability were monitored using Mn^{2+} quench of Fura-2 fluorescence as previously described (Harper *et al*., 2007). Changes in extracellular $[Ca^{2+}]$ ($[Ca^{2+}]_{ext}$) were monitored using washed platelets resuspended in the presence of 2.5 µM Fluo-3 or Fluo-4, or 5 µM Rhod-5N K^+ salt (Sage *et al*., 2013). Cells were preincubated with

nicergoline, taxol, or their vehicle, DMSO under magnetic stirring at 37°C. Fluorescence was recorded from 1.2 mL stirred aliquots of platelet suspension at 37°C using a Cairn Research Spectrophotometer (Cairn Research, Faversham, U.K.). Fluorescence readings were corrected for fluorescent effects of taxol both alone and in the presence of nicergoline. $[Ca^{2+}]_{cyt}$, $[Ca^{2+}]_{ext}$, $[Ca^{2+}]_{peri}$ and $[Ca^{2+}]_{st}$, were quantified by integration of the change in fluorescence records from basal with respect to time for 3.5 min after thrombin addition.

Single platelet imaging

Fixed platelet samples for the antibody-mediated labelling of KDEL-containing proteins were produced by treating unstimulated, washed human platelets with either 100 µM nicergoline or its vehicle, DMSO, for 5 minutes at 37°C. Cells were then fixed by addition of 3% [w/v] formaldehyde and stored at 4°C until use. Platelets were collected by centrifugation and then permeabilised by incubation in Phosphate-buffered saline (PBS) containing 0.1% Triton X-100 and 1 $mg.mL^{-1}$ bovine serum albumin (BSA) for 10 minutes at room temperature. Cells were recollected by centrifugation and resuspended in PBS containing a 1:100 dilution of the anti-KDEL antibody and 1 $mg.mL^{-1}$ BSA and incubated at room temperature for 30 minutes. Cells were recollected by centrifugation and finally resuspended in PBS containing 1 $mg.mL^{-1}$ BSA.

Platelet microtubule structure was monitored in cells co-loaded with 5 µM Fura-red/AM for 45 minutes and 500 nM Tubulin tracker for 30 minutes at 37°C in PRP (Diagouraga *et al*., 2013; Sage *et al*., 2011). After dye loading cells were washed by centrifugation and resuspended in supplemented HBS. For Fluo-4 imaging, 2.5 µM Fluo-4 salt was added immediately prior to imaging (Sage *et al*., 2013). Cells were preincubated with 100 µM nicergoline (or its vehicle, DMSO) under magnetic stirring for 5 minutes at 37°C. Chambered slides (Ibidi µ-slide 8 well) were coated with a poly-L-lysine solution (Sigma Aldrich, UK) overnight at 4°C. Slides were washed with supplemented HBS, or PBS (KDEL antibody experiments only) and mounted on the microscope stage. Appropriately-labelled platelet suspensions at a density of 2×10^8 mL^{-1} were pipetted into the chambered coverslip and allowed to adhere to the substrate for 3 min. Excess platelet suspension was then removed and the slides washed twice with supplemented HBS to which 1 mM EGTA was added or PBS (KDEL antibody experiments only). Fluorescence was monitored using a Fluoview FV1200 laser-scanning confocal microscope (Olympus, U.K.) with a PLAPON 60× oil immersion objective. Images were recorded at a frequency of 0.5 Hz for 5 min with excitation at 473 nm (Fluo dyes, anti-KDEL antibody and TubulinTracker) or 543 nm (Fura Red and CytoPainter Phalloidin iFluo555) and emission at 490–520 nm or 590-620nm respectively.

Dense granule secretion

Dense granule secretion was monitored using our previously reported methodology (Harper *et al*., 2009). Briefly, luciferin–luciferase (1% [v/v] final concentration) was added to 1.5 mL stirred aliquots of platelets prior to the start of experiments, and thrombin-evoked changes in light emitted were monitored using a high-gain photomultiplier tube. Measurements of ATP secretion were taken as the integral over basal readings (mean value for 30 sec before stimulation) for 3 minutes after stimulation.

Group sizes

Group sizes are equal for all experiments. *n* denotes independently tested platelet samples taken from blood provided by 3-5 donors.

Randomization

Samples were tested in time-matched groups of control and treated samples, to ensure that time-dependent degradation of platelet responsiveness did not affect the results. Control and treated samples were randomly assigned to samples within each of these groups prior to the start of the experiment.

Blinding

Data files were labelled with a date and sample identifier (e.g. letter, number or time of experiment). Data were analysed in this format and then subsequently reassigned to their experimental condition using lab records.

Normalization

Data were subjected to statistical analysis prior to normalisation. Data sets are presented as Mean % of control to allow for comparison of results obtained between different preparations, in which there can be significant variation in the magnitude of agonist-evoked Ca^{2+} signals observed in the control responses of samples taken from different donors.

Mn^{2+} quench experiments use normalisation to baseline fluorescence levels (F/F_0) to allow for differences in resting Fura-2 fluorescence of samples.

Statistical Comparison

Values are stated as the mean ± SEM of the number of independent observations (n) indicated. Analysis of statistical significance was performed on independently-acquired values using a paired Student's t-test or using a one-way ANOVA test followed by a post hoc Bonferroni multiple comparisons test. $P < 0.05$ was considered significant.

Results

Nicergoline inhibits thrombin-evoked Ca^{2+} signalling in human platelets.

Experiments were performed to examine whether pretreating platelets with nicergoline at a concentration able to trigger reorganisation of the OCS and DTS (Le Menn *et al*., 1979) affected Ca^{2+} signalling. These experiments were initially performed in the absence of extracellular Ca^{2+}, as these conditions allow the clearest examination of pericellular Ca^{2+} recycling by preventing direct Ca^{2+} entry through channels in the plasma membrane. As shown in Figure 2A, preincubation with 10 µM nicergoline for 10 minutes at 37°C had no effect on thrombin-evoked rises in $[Ca^{2+}]_{cyt}$ (100.6% ± 7.9% of control; $n = 6$; $P > 0.05$), whereas pretreatment with 50 µM or 100 µM nicergoline elicited a significant inhibition of thrombin-evoked rises in $[Ca^{2+}]_{cyt}$ (Figure 2B; 84.1% ± 3.1% and 74.4% ± 4.3% of control for 50 µM and 100 µM respectively; both $n = 6$; $P < 0.05$). In addition, pretreatment with

higher concentrations of nicergoline was found to elicit a small, but significant fall in the resting $[Ca^{2+}]_{cyt}$ observed after EGTA treatment (Figure 2C; 48.3 ± 2.6 nM and 38.8 ± 0.9 nM for 50 µM and 100 µM respectively; both $n = 6$; $P < 0.05$) compared to the control samples (64.6 ± 2.6 nM; n = 6). No significant effect on resting $[Ca^{2+}]_{cyt}$ was observed in cells pretreated with 10 µM nicergoline (57.8 ± 2.0 nM; n = 6; $P > 0.05$). Further experiments found that nicergoline itself induced no change in $[Ca^{2+}]_{cyt}$ either in the presence or absence of external Ca^{2+} , but it did trigger a slow, small reduction in the baseline measured Ca^{2+} (Supplementary Figure 1).

Pretreatment of platelets with 100 µM nicergoline also significantly inhibited thrombin-evoked release of Ca^{2+} from intracellular stores (73.9% ± 4.9% of control; $n = 5$; $P < 0.05$; Figure 2D). However unlike $[Ca^{2+}]_{cyt}$, baseline Fluo-5N fluorescence was found to be unaffected by nicergoline treatement (101.8% ± 3.1% of control; $n = 5$; $P > 0.05$). These results demonstrate that nicergoline reduces thrombin-stimulated increases in $[Ca^{2+}]_{cyt}$, through reducing thrombin-evoked release of Ca^{2+} from intracellular stores, and not by changing their basal Ca^{2+} content. In addition the lack of change in resting $[Ca^{2+}]_{st,}$ suggests that the nicergoline-induced reduction in $[Ca^{2+}]_{cyt}$ is not mediated through increasing Ca^{2+} uptake into the intracellular Ca^{2+} stores.

Given the nicergoline concentrations utilised here are significantly higher than those required to fully inhibit α-adrenoreceptors, it seems most likely that the inhibitory effect of nicergoline on resting and thrombin-evoked Ca^{2+} signalling is related to the ultrastructural reorganisation of the platelets previously reported (Le Menn *et al*., 1979).

Nicergoline causes disruption to the cortical microtubule network

Le Menn *et al.*, (1979) demonstrated that nicergoline treatment results in reorganisation of the platelet cortical microtubule bundle, with the bundle remaining present but with an apparent reduction in the number of microtubules, with the remainder displaced centrally. The authors also reported that reorganisation of the cortical microtubule bundle also caused the cells to become more spherical, in line with the known role of this cytoskeletal structure in maintaining platelets in their resting discoid form (Italiano *et al*., 2003).

To confirm that nicergoline causes disorganisation of the cortical microtubule network, the microtubule structure of nicergoline- and DMSO-treated platelets was examined in resting platelets co-loaded with both TubulinTracker and the cytosolic label, Fura red. Platelets treated with DMSO (the vehicle for nicergoline) frequently had prominent cortical bundles of microtubules with only weak fluorescence observed from the central regions of the cells (Figure 3). In contrast, platelets treated with 100 µM nicergoline were found to have a significant disruption to the cortical microtubule bundle with a greater percentage of platelets in each field demonstrating a complete lack of a discernible cortical bundle (24.5% ± 7.4% of nicergoline-treated platelets compared to 11.2% ± 5.2% of DMSO-treated platelets ; $n = 9$; $P < 0.05$) or showing an incomplete cortical ring (21.0% ± 2.9% of nicergoline-treated platelets compared to 9.2% ± 3.6% of DMSO-treated platelets; $n = 9$; $P < 0.05$). A reduced proportion of the TubulinTracker fluorescence was observed in the cortical regions in nicergoline-treated platelets (63.9% ± 5.1% in DMSO-treated platelets compared to 36.3% ± 6.4% in nicergoline-treated platelets ; $n = 9$; $P < 0.05$). Nicergoline pretreatment also reduced the thickness of the microtubule bundles in cells displaying an observable cortex (197 nm ± 50 nm in nicergoline-treated platelets compared to 401 ± 64 nm in DMSO-treated platelets; $n = 9$; $P < 0.05$). These results confirm the findings of Le Menn *et* al. (1979) that nicergoline pretreatment disrupts the structure of the cortical microtubule bundle.

In addition, experiments were performed to examine the effect of nicergoline on the actin cytoskeleton in fixed cells. Although no obvious difference was seen in the morphology of live nicergoline-treated cells plated onto poly-L-lysine-coated coverslips, when experiments were performed using fixed cells the nicergoline-treated cells could be observed to take a consistent rounded form (Supplementary Figure 2) – consistent with them becoming more spherical in shape. The observation that fixed nicergoline-treated platelets plated onto coverslips appear spherical, whilst live cells appear similar to the control cells, suggests that platelets are able to spread similarly to control cells through remodelling of their cortical F-actin layer. Further analysis of these cells found that nicergoline caused a slight thickening of the cortical actin ring without altering the amount of F-actin within the cells. These data are presented and discussed further in the Supplementary materials (Supplementary Figure 2)

Nicergoline triggers a reorganisation of the dense tubular system and inhibits thrombin-evoked Ca^{2+} removal and pericellular Ca^{2+} accumulation in human platelets

Le Menn *et al*. (1979) demonstrated that high concentrations of nicergoline cause a reorganisation of the membrane of the DTS, with these intracellular Ca^{2+} stores remaining associated with the disorganised microtubule system. Experiments were therefore performed to assess the effect of nicergoline on the subcellular localisation of the DTS. To confirm the nicergoline-induced change in the DTS, fixed nicergoline or DMSO-treated platelets were permeabilised and stained using an antibody to proteins containing the endoplasmic reticulum retention signal, KDEL. This approach has previously been used to demonstrate the specific localisation of Protein Disulfide Isomerase (PDI) in the DTS (van Nispen tot Pannerden *et al*., 2009). Fluorescent imaging of the labelled cells found that control cells possessed an inhomogeneous, punctate distribution (Figure 4A) – which is consistent with previous observations of the distribution of PDI in human platelets (van Nispen tot Pannerden *et al*., 2011). In contrast nicergoline-treated cells, did not show such obvious puncta and fluorescence appeared to be more homogenously distributed. This was confirmed in line scan analysis of the cells, with DMSO-treated cells showing 1 or 2 obvious spikes in the fluorescence levels in localised areas of the cell (Figure 4B), in contrast nicergoline-treated cells did not show such spikes and were instead seen to have a homogenous fluorescence in their interior, with fluorescence only falling at the cell margins. Quantitative analysis of these results found that mean cellular fluorescence was unaffected by nicergoline pretreatment (97.3% ± 4.6% of control; $n = 5$; $P > 0.05$; Figure 4), yet the variance in platelet pixel fluorescence was found to be significantly lower in nicergoline-treated platelets (Standard deviation = 451.5 ± 24.4 arbitrary units in nicergoline-treated cells compared to 565.6 ± 312 arbitrary units in DMSO-treated cells; n = 5; $P < 0.05$). The maximum cell pixel fluorescence in nicergoline-treated platelets was also found to be consistently reduced across all donors (82.4% ± 4.1% of control; $n = 5$; $P < 0.05$). These data suggest that there is no difference in DTS content of nicergoline-treated platelets, but the DTS is redistributed away from its normal concentration at the membrane complex. Similar effects of nicergoline upon the distribution of intracellular Ca^{2+} stores was also observed in Fluo-5N-loaded human platelets (Supplementary Figure 3). These results are consistent with previous work that indicates that the cortical microtubule bundle is likely to be important in maintaining the normal inhomogenous distribution of the DTS in platelets (Le Menn *et al*., 1979; White, 1968).

Our previous work has indicated that the close interaction of membranes at the MC is required for the near-maximal rate of thrombin-evoked Ca^{2+} efflux, and calculated that this high rate of transport would be needed to generate the observed thrombin-evoked pericellular Ca^{2+} signals (Sage *et al*., 2013). Experiments were therefore performed to examine whether

the nicergoline-induced redistribution of the intracellular Ca^{2+} stores affected Ca^{2+} removal from the cell and accumulation in the pericellular space. As shown in Figure 5A,B, nicergoline treatment significantly inhibited thrombin-evoked Ca^{2+} efflux from the cells (37.1% ± 3.9% of control; n = 5; P < 0.05; Figure 5) and also inhibited the resulting increase in $[Ca^{2+}]_{peri}$ (23.3% ± 8.4% of control; n = 6; P < 0.05; Figure 5), suggesting that reorganisation of the intracellular membranes may affect thrombin-evoked rises in $[Ca^{2+}]_{cyt}$ by interfering with pericellular Ca^{2+} recycling by inhibiting Ca^{2+} removal into the pericellular space by disrupting the close apposition of the DTS with the OCS. This conclusion was supported by additional experiments showing that nicergoline induces no additional inhibitory effect when pericellular Ca^{2+} rises are also blocked (Supplemental Figure 4).

Interestingly, there was no significant alteration observed in either the resting $[Ca^{2+}]_{ext}$ or $[Ca^{2+}]_{peri}$ (99.8% ± 4.7% and 98.6% ± 12.1% of control for $[Ca^{2+}]_{ext}$ and $[Ca^{2+}]_{peri}$ respectively; n = 5 and 6 respectively; P > 0.05 for both). As the data indicates that nicergoline induces no active redistribution of Ca^{2+} from either the extracellular fluid, nor the intracellular stores – these results suggest that the most likely reason for the nicergoline-induced reduction in resting $[Ca^{2+}]_{cyt}$ is a small increase in the cytosolic volume caused by the loss of the cortical microtubule bundle leading to platelet become more spherical in shape. Given that platelets rapidly change shape from discoid to spherical upon activation, such a change in cell volume is unlikely to significantly alter thrombin-evoked Ca^{2+} signals.

Stabilisation of platelet microtubules by prior treatment with taxol prevents nicergoline-induced disruption of thrombin-evoked Ca^{2+} signalling in platelets.

As the nicergoline-induced ultrastructural changes in the DTS and OCS appear to be related to a change in the cortical microtubule structure (Le Menn *et al*., 1979), further experiments were performed to investigate whether preventing microtubule reorganisation by pre-treatment of platelets with the microtubule-stabilising agent, taxol, prior to incubation with nicergoline negated the inhibitory effect of nicergoline on thrombin-evoked Ca^{2+} signalling. As previously observed, pretreatment with nicergoline significantly inhibited thrombin-evoked rises in $[Ca^{2+}]_{cyt}$ to 64.6% ± 5.1% of control (n = 7; P < 0.05; Figure 6A). In contrast, incubation of taxol-pretreated platelets with nicergoline resulted in no significant defect in the thrombin-evoked rise in $[Ca^{2+}]_{cyt}$ compared to the taxol-pretreated cells (107.2% ± 7.0% of control; n = 7; P > 0.05). In line with a role for the nicergoline-induced structural alterations in eliciting the reduced resting $[Ca^{2+}]_{cyt}$ previously observed, we find that whilst nicergoline alone again triggered a reduction in $[Ca^{2+}]_{cyt}$ (35.0 ± 8.8 nM for nicergoline-treated vs 50.8 ± 5.6 nM for control cells; n = 7; P < 0.05), when cells were treated with taxol prior to nicergoline, there was no significant difference in the observed resting $[Ca^{2+}]_{cyt}$ (98.3 ± 17.2 nM for nicergoline- and taxol-treated cells vs 80.6 ± 20.3 nM for taxol-treated cells; n = 7; P > 0.05).

Similar experiments were performed to examine whether taxol pretreatment also prevented the effect of nicergoline on thrombin-evoked changes in $[Ca^{2+}]_{st}$, $[Ca^{2+}]_{ext}$ and $[Ca^{2+}]_{peri}$. Consistent with the previous experiments, nicergoline significantly inhibited thrombin-evoked changes in $[Ca^{2+}]_{st}$ (52.4% ± 8.3% of control; n = 8; P < 0.05; Figure 6B), $[Ca^{2+}]_{ext}$ (41.0% ± 16.6% of control; n = 10; P < 0.05; Figure 6C), and $[Ca^{2+}]_{peri}$ (11.0% ± 11.0% of control; n = 7; P < 0.05; Figure 6E). However upon pretreatment with taxol, nicergoline had no statistically significant effect on any of these parameters (81.3% ± 12.9% of control, 86.0% ± 20.7% of control and 263.3% ± 99.8% of control for $[Ca^{2+}]_{st}$, $[Ca^{2+}]_{ext}$ and $[Ca^{2+}]_{peri}$ respectively; n = 8, 10 and 7 respectively; P > 0.05 for all conditions; Figure 6B,D,F). These data indicate that nicergoline-induced changes in Ca^{2+} signalling are due to the structural

alteration induced by disruption of the cortical microtubule bundle, likely resulting in disruption of the MC.

Nicergoline treatment inhibits the initial accumulation and spread of Ca^{2+} from the pericellular Ca^{2+} hotspot

Single cell imaging was employed to examine whether nicergoline treatment alters the characteristics of the pericellular Ca^{2+} accumulations observed in single platelets. As previously shown, virtually all DMSO-treated platelets were observed to generate a pericellular Ca^{2+} hotspot within the platelet boundary upon thrombin stimulation (e.g. as indicated by yellow arrow in Figure 7B; 93.5% ± 3.1% of cells/field, n = 5; Sage *et al*., 2013). Whilst most nicergoline-treated platelets were still able to generate a similar microdomain of raised $[Ca^{2+}]_{peri}$, the proportion of cells showing a Ca^{2+} hotspot was significantly reduced (62.9% ± 7.6% of cells/field in treated cells; n = 5; P<0.05). The thrombin-evoked increase in the fluo-4 fluorescence observed in the hotspots was found to be significantly reduced in nicergoline-treated platelets compared to control cells (30.1% ± 8.9% of control ; n = 5; P < 0.05). In addition, we confirmed our previous observation that the Ca^{2+} could often be seen to diffuse strongly away from the initial hotspots of pericellular Ca^{2+} accumulation in a directionally-restricted manner through either a portion of the cell or around the platelet cortical region to the opposite half of the platelet (Sage *et al*., 2013). In contrast, pericellular Ca^{2+} spread was less frequently seen in nicergoline-treated platelets, with Ca^{2+} only infrequently spreading to the opposite side of the cell (observed in 20.9 ± 3.4% of cells/field in treated cells compared to 49.9% ± 3.2% of cells/field in DMSO-treated cells; n = 5; P < 0.05). We also observed that the pericellular hotspot was generally more dispersed in nicergoline-treated platelets (1.7 ± 0.7 μm^2 in nicergoline-treated cells compared to 0.6 ± 0.2 μm^2 in control cells; both n = 5), although this was not found to be statistically significant (P > 0.05).

These results indicate that the nicergoline-induced redistribution of the DTS reduces Ca^{2+} accumulation within the pericellular hotspot, and is consistent with the hypothesis that the MC is responsible for the efficient accumulation of Ca^{2+} at the pericellular Ca^{2+} hotspot.

Pretreatment with taxol partially reverses the inhibitory effect of nicergoline on thrombin-evoked dense granule secretion

Previously we have demonstrated a role for pericellular Ca^{2+} recycling in potentiating dense granule secretion from thrombin-stimulated cells (Sage *et al*., 2013). Experiments were performed to investigate whether nicergoline inhibits dense granule secretion. As shown in Figure 8A, nicergoline pretreatment almost completely ablated thrombin-evoked dense granule secretion (15.1% ± 3.6% of control; n = 6; P < 0.05). In contrast to our finding with thrombin-evoked Ca^{2+} signalling, taxol pretreatment only partially reversed the inhibitory effect of nicergoline on granule secretion, with a partial inhibition still observed (67.0% ± 8.6% of control; n = 6; P < 0.05). These data therefore suggest that reversing the effects of nicergoline on pericellular Ca^{2+} recycling restores a significant dense granule secretion, in line with our previous data suggesting that pericellular Ca^{2+} recycling provides a secondary Ca^{2+} source which potentiates dense granule secretion (Sage *et al*., 2013). However there is also a taxol-insensitive effect of nicergoline on dense granule secretion suggesting that there is a secondary action of this drug which prevents secretion even in the presence of normal pericellular Ca^{2+} recycling.

Further experiments were performed to examine whether niceegoline's inhibition of dense granule secretion could be the cause, and not the consequence, of nicergoline's inhibition of thrombin-evoked Ca^{2+} signalling. These data suggested that nicergoline's effect on thrombin-

evoked Ca^{2+} signalling occurred upstream of to its effect on dense granule secretion (Supplementary Figure 5).

Pretreatment with taxol partially reverses the inhibitory effect of nicergoline on thrombin-evoked Ca^{2+} signalling elicited when platelets are stimulated in the presence of extracellular Ca^{2+}

Experiments were also performed to examine whether nicergoline inhibits thrombin-evoked Ca^{2+} signalling in the presence of extracellular Ca^{2+}. As shown in Figure 9A, pretreatment of platelets with nicergoline significantly inhibited thrombin-evoked rises in $[Ca^{2+}]_{cyt}$ in the presence of 1 mM extracellular Ca^{2+} (31.5% ± 5.1% of control; n = 13; $P < 0.05$; Figure 9). However unlike most of the other findings above, taxol pretreatment was not able to fully prevent the inhibitory effects of nicergoline on thrombin-evoked Ca^{2+} signalling (58.9% ± 8.9% of control; n = 13; $P < 0.05$). Interestingly this inability of taxol to fully reverse the inhibitory effect of nicergoline appeared to be related to an inability of the cells to maintain the prolonged, secondary plateau phase of the Ca^{2+} signal, as the initial $\Delta[Ca^{2+}]_{cyt}$ in the initial spike phase of the Ca^{2+} response was not affected by nicergoline in taxol pre-treated cells (101.2% ± 14.5% of control; n = 13; $P > 0.05$). However the inhibitory effect on the plateau elicited by nicergoline treatment caused the integral of the full Ca^{2+} signal to be inhibited (51.1 ± 4.3% of control; n = 13; $P < 0.05$).

Examination of the individual Ca^{2+} fluxes which contribute to the rise in $[Ca^{2+}]_{cyt}$ showed that in the presence of extracellular Ca^{2+}, nicergoline significantly inhibited thrombin-evoked removal of Ca^{2+} from the cell (18.9% ± 10.6% of control; n = 9; $P < 0.05$), Ca^{2+} release from intracellular stores (59.8 ± 6.1% of control; n = 8; $P < 0.05$) and initial opening of Ca^{2+}-permeable ion channels as assessed by Mn^{2+} quench of Fura-2 fluorescence (40.0% ± 6.5% of control; n = 8; $P < 0.05$). However, pretreatment with taxol prevented nicergoline from eliciting a statistically significant effect on each of these component Ca^{2+} fluxes (83.9% ± 24.7%, 115.3% ± 27.0% and 81.3% ± 12.8% of control respectively ; n = 9, 8 and 8 respectively; all $P > 0.05$). These results suggest that pericellular Ca^{2+} recycling at the MC is required to potentiate the maximum amplitude of the initial thrombin spike by facilitating Ca^{2+} release and Ca^{2+} entry (probably by facilitating store depletion and thus triggering store-operated Ca^{2+} entry; Figure 8; Braun *et al*., 2008; Sage *et al*., 2013), however nicergoline has taxol-insensitive effects on the plateau phase which prevents the full reinstatement of the Ca^{2+} signal seen under these conditions. Previous work on platelets from patients with storage pool disorder has demonstrated that the plateau phase of thrombin-evoked Ca^{2+} responses requires the maintained opening of receptor-operated channels triggered by the secretion of ATP, ADP and 5-HT from the dense granules (Lages and Weiss, 1999). Given the observed taxol-insensitive effects on dense granule secretion (Figure 8) and the effect only being observed in the presence of extracellular Ca^{2+}, we suggest the possibility that nicergoline prevents autocrine-dependent signalling either via an inhibitory effect on secretion or via an inhibitory effect on a downstream receptor or channel.

Discussion

In our previous work we hypothesised that the nanojunction created at the membrane complex played a key role in platelet function by regulating Ca^{2+} release from intracellular stores (Sage *et al*., 2013). In this paper, we have demonstrated that nicergoline-induced disruption of platelet ultrastructure results in analogous inhibitory effects on thrombin-evoked Ca^{2+} signalling as previously reported for a range of experimental manipulations that prevented pericellular Ca^{2+} recycling (Sage *et al*., 2013). Previously we used a quantitative analysis of our Ca^{2+} signalling data to demonstrate that the creation of a pericellular Ca^{2+}

hotspot was most likely due to the action of the MC. Here we demonstrate that disruption of the normal organisation of the OCS and DTS by nicergoline also disrupts the creation of this highly-concentrated pericellular Ca^{2+} hotspot. These results therefore support our hypothesis that the MC may be responsible for the creation of the pericellular Ca^{2+} hotspot.

Le Menn *et al*. (1979) previously suggested that the change in distribution of the two component membrane systems of the MC appeared to be due to disruption of the cortical microtubule system. In line with this, we have demonstrated that pre-treatment of platelets with taxol reverses the majority of the effects of nicergoline on thrombin-evoked Ca^{2+} signalling. In addition, previous studies have also shown that the microtubule-disrupting agent colchicine was able to elicit a reduction in thrombin-evoked Ca^{2+} release to about 80% of control (Redondo *et al*., 2007). This effect is similar in magnitude to that observed using nicergoline, and suggests that normal microtubule structure is required to elicit normal Ca^{2+} signalling in human platelets. These data suggest that the cortical microtubule bundle is likely to play a role in scaffolding the nanojunctions created by the close apposition of the OCS and DTS. This is supported by previous electron microscope studies performed by Behnke (1967) and White (1968; 1972), who both showed an association of DTS, OCS and cortical microtubules at the MC. Further investigations will need to examine how nicergoline is able to disrupt microtubule structure. Recent work by Sadoul and co-workers has suggested a number of possible mechanisms, including an alteration in the activity of microtubule associated molecular motors such as myosin, kinesin and dynein, as well as the possibility of destabilising the microtubule bundle through altering the post-translational modifications of tubulin (e.g acetylation or detyrosination; Diagouraga *et al*., 2013; Sadoul *et al.*, 2012).

Given the ability of high concentrations of nicergoline to inhibit Ca^{2+} signalling as well as agonist-evoked platelet adhesion, secretion and aggregation (Lanza *et al*., 1986), we hypothesise that the MC plays a key role in amplifying platelet Ca^{2+} signals and modulating platelet activation. This hypothesis is supported by a number of clinical case reports which have demonstrated that patients with abnormal membrane complexes suffer from bleeding disorders (Canizares *et al*., 1990; Green *et al.*, 1981; Meiamed *et al*., 1984; Parker *et al*., 1993). Of particular note here is one report in which an inherited MC defect was found to be related to a deficit in thrombin-evoked Ca^{2+} signalling (Parker *et al*., 1993), in line with our findings presented here.One limitation of our current findings is that nicergoline was also found to have a secondary taxol-insensitive effect on dense granule secretion (Figure 8). These data suggest that nicergoline can also inhibit dense granule secretion by a mechanism beyond its effect on pericellular Ca^{2+} recycling (Figure 10). From the data provided here, it seems most likely that either nicergoline's effect on the cortical actin cytoskeleton, or a possible effect on dense granule motility may account for the taxol-insensitive secretory defect observed. As previous studies have shown that using jasplakinolide to induce actin polymerisation and thickening of the cortical actin ring can also reduce dense granule secretion (Cerecedo *et al*., 2010), it is possible that the nicergoline-induced thickening of the cortical actin cytoskeleton might underlie the taxol-insensitive effects on granule secretion. Alternatively, it is possible that nicergoline could directly or indirectly inhibit the activity of a molecular motor which could elicit a reorganisation of the cortical microtubule bundle as well as affecting agonist-induced platelet granule motility. For example, previous work has suggested that kinesin may play an important role in mediating platelet granule motility (Cerecedo *et al*., 2010), as well as in maintaining normal cortical microtubule bundle shape (Diagouraga *et al*., 2014). If nicergoline works through the inhibition of a molecular motor such as kinesin, this might potentially account for both the taxol-dependent and taxol-independent effects of nicergoline. Further work will be needed to examine whether it is

possible to separate out the taxol-sensitive and insensitive aspects of nicergoline on platelet function.

Conclusion

From the data presented here and elsewhere (Lanza *et al*., 1986; Le Menn *et al*., 1979), we suggest that nicergoline provides an initial proof-of-concept that a MC-disrupting drug could be developed and would be effective as an anti-thrombotic. We propose that by studying the molecular mechanisms by which nicergoline interferes with the platelet ultrastructure, we may be able to better understand the molecular structures underlying the formation of the MC. As such, nicergoline may be useful as a prototype compound which can be used to help identify new pharmacological targets for the development of more selective MC-disrupting drugs.

Funding Information

TW was supported by a Vacation Studentship from The Physiological Society. FM was supported by a PhD studentship from the British Heart Foundation (FS/12/48/29719). AGSH was supported by a research grant from the Physiological Society.

Acknowledgements

We would like to thank Dr Stewart Sage and Dr Mike Mason for their help in performing the dense granule secretion assays, as well as for valuable discussions of the data presented here

Conflict of Interests

The authors declare they have no conflict of interests to disclose.

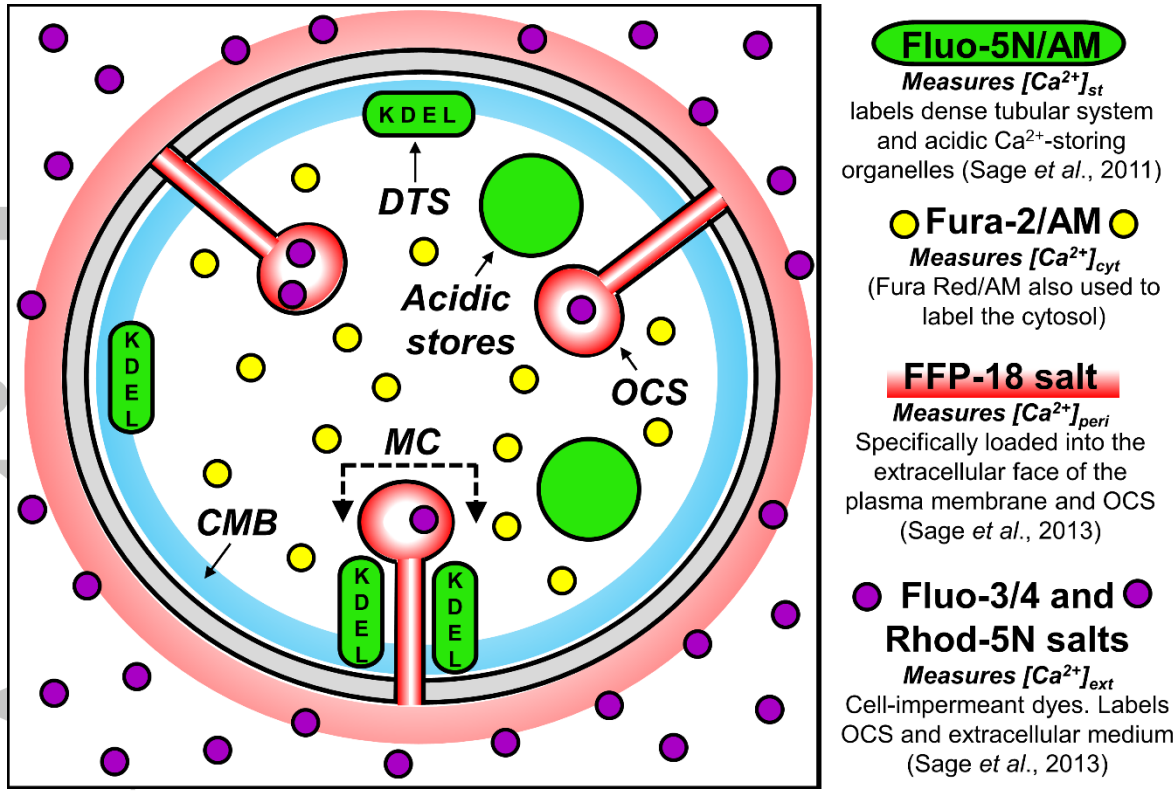

Figure 1. A summary of the localisation of fluorescent Ca^{2+} indicators used in this study. The diagram shows a simplified structural diagram of a platelet including key cellular structures discussed in this paper. These include the dense tubular system (DTS; the platelet equivalent of the smooth endoplasmic reticulum), the open canalicular system (OCS; a complex invagination of the platelet plasma membrane), the membrane complex (MC; a close apposition of the OCS and DTS), the cortical microtubule bundle (CMB; made up of a number of microtubule coils; Labelled with TubulinTracker) and the acidic Ca^{2+} stores (which likely encompass the lysosomes as well as the α- and dense granules). Note the presence of KDEL-containing proteins solely within the DTS (van Nispen tot Pannerden *et al*., 2009), which allows this structure to be labelled distinctly from the acidic Ca^{2+} stores. A cortical actin ring is also found in platelets and occupies a space similar to the cortical microtubule bundle (labelled with CytoPainter Phalloidin-iFluor555).

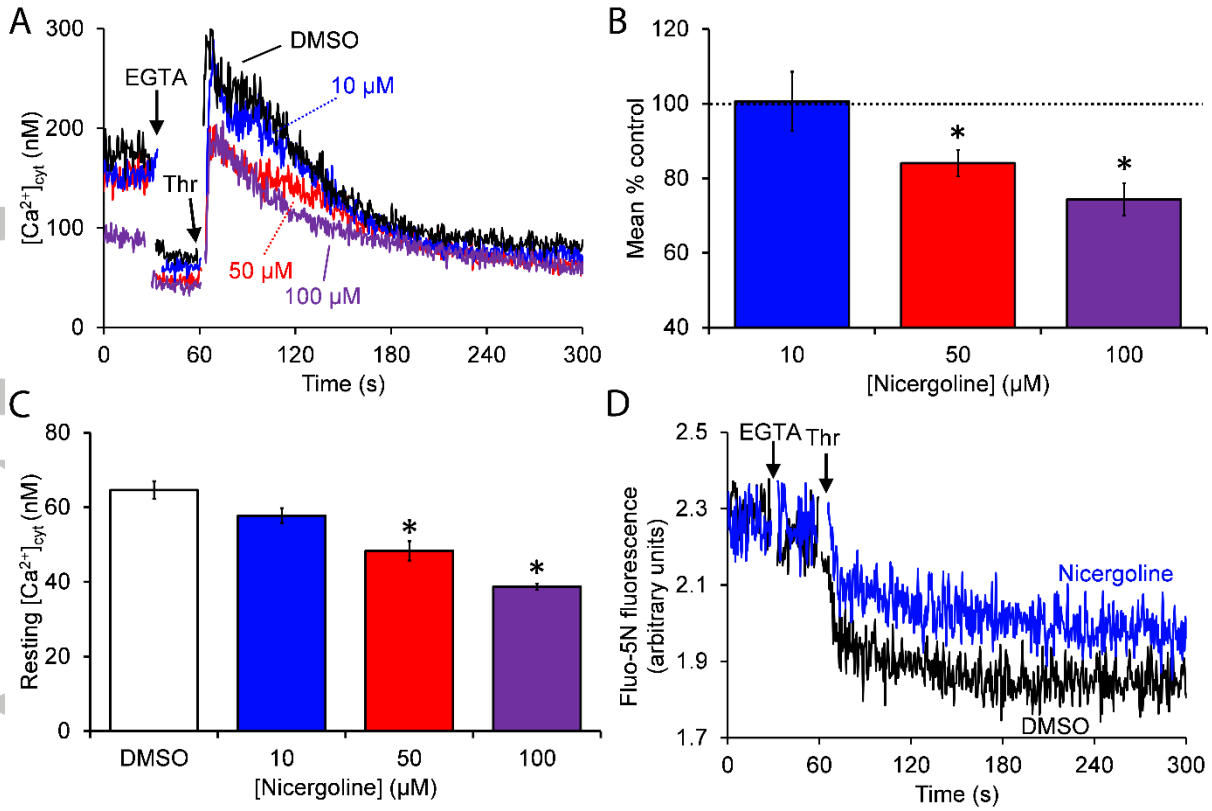

Figure 2: Nicergoline inhibits resting and thrombin-evoked Ca^{2+} signalling in human platelets. Fura-2- (A-C) or Fluo-5N-loaded (D) human platelets were suspended in supplemented HBS. Platelets were pre-treated with 10, 50 or 100 µM nicergoline for 10 min at 37°C in the presence of continuous magnetic stirring. 1 mM EGTA was added before the cells were stimulated with 0.5 $U.mL^{-1}$ thrombin. (B,C) show graphs summarising the effect of nicergoline on thrombin-evoked changes in $[Ca^{2+}]_{cyt}$ (B) and resting $[Ca^{2+}]_{cyt}$ (C) respectively. Results presented are representative of 6 and 5 experiments respectively.

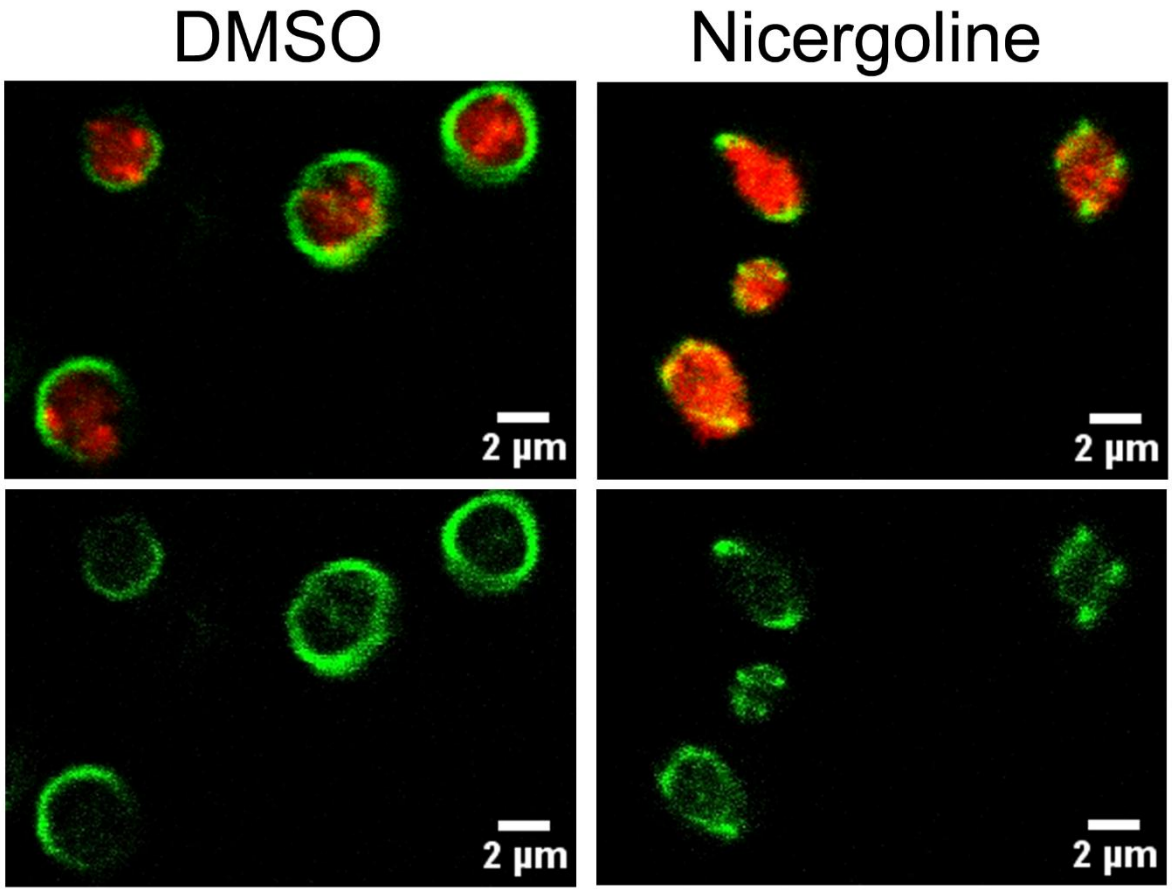

Figure 3. Nicergoline causes disruption of the cortical microtubule network (A) Platelets co-loaded with both TubulinTracker and Fura Red were suspended in supplemented HBS. Cells were pretreated with either DMSO or 100 µM nicergoline for 5 min at 37°C in the presence of continuous magnetic stirring. The platelets were then added to a poly-L-lysine-coated chambered slide, and allowed to settle for 3 minutes. Excess platelet suspension was removed and the slides were washed twice with Ca^{2+}-free HBS. Fluorescence was then monitored using an Olympus Fluoview FV1200 confocal microscope. The upper panels show the overlay of both TubulinTracker and Fura Red fluorescence; the lower panels show the fluorescence from TubulinTracker alone. The results presented are representative of 9 experiments.

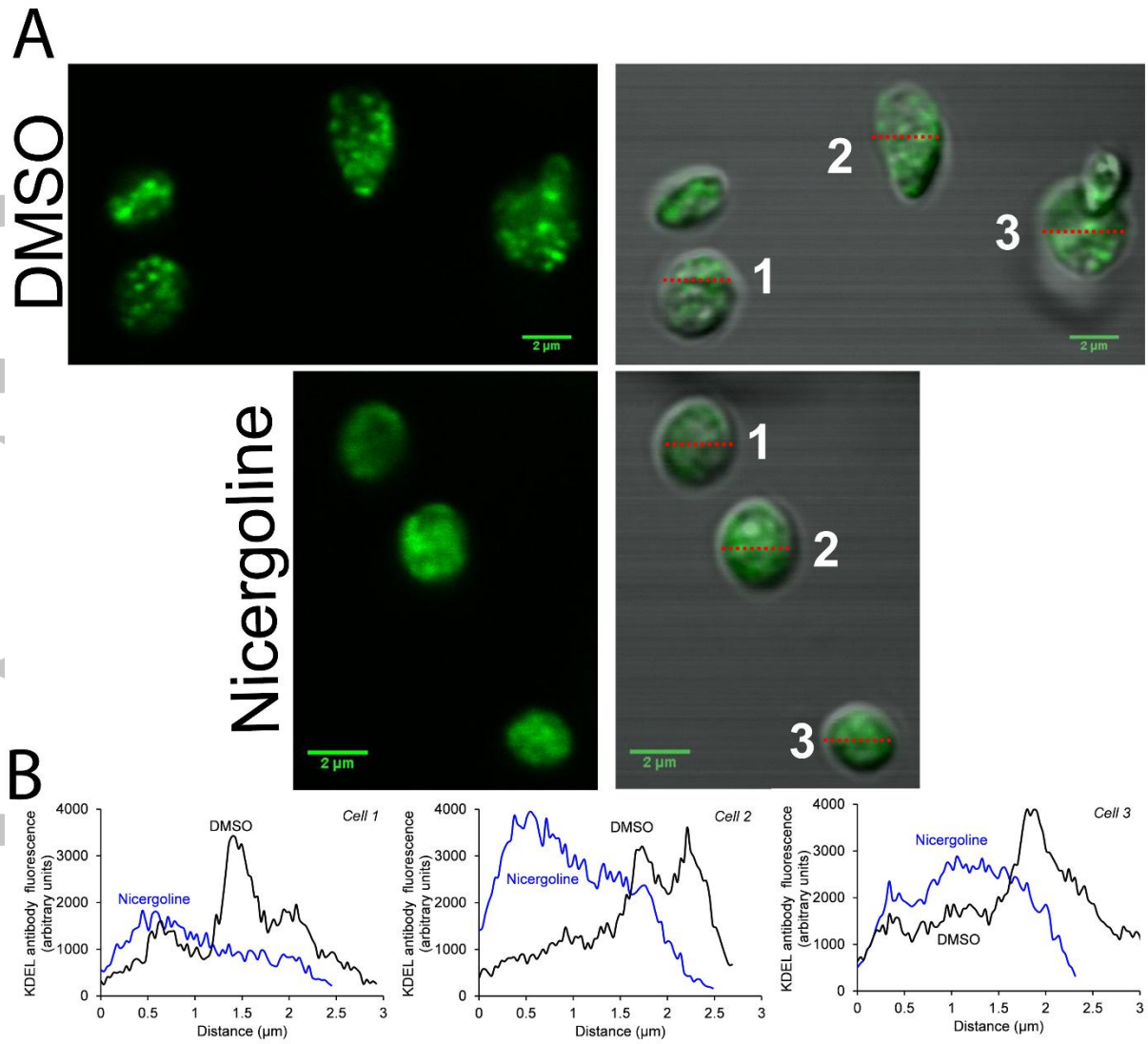

Figure 4. Nicergoline triggers redistribution of the DTS (A) Platelets were treated with either DMSO or 100 µM nicergoline for 5 min at 37°C in the presence of continuous magnetic stirring. Cells were then fixed, permeabilised and incubated with 1% [v/v] Fluor®488-labelled anti-KDEL antibody for 30 minutes at room temperature. The cells were washed and then resuspended in supplemented HBS. The labelled cells were then allowed to settle for 3 minutes on poly-L-lysine-coated chambered slide. Fluorescence was then monitored using an Olympus Fluoview FV1200 confocal microscope. Images for the fluorescence alone (left) or overlaid over the transmitted light image (right) are shown. (B) A linescan analysis of the 3 numbered cells indicated in (A) are shown. The results presented are representative of 5 experiments.

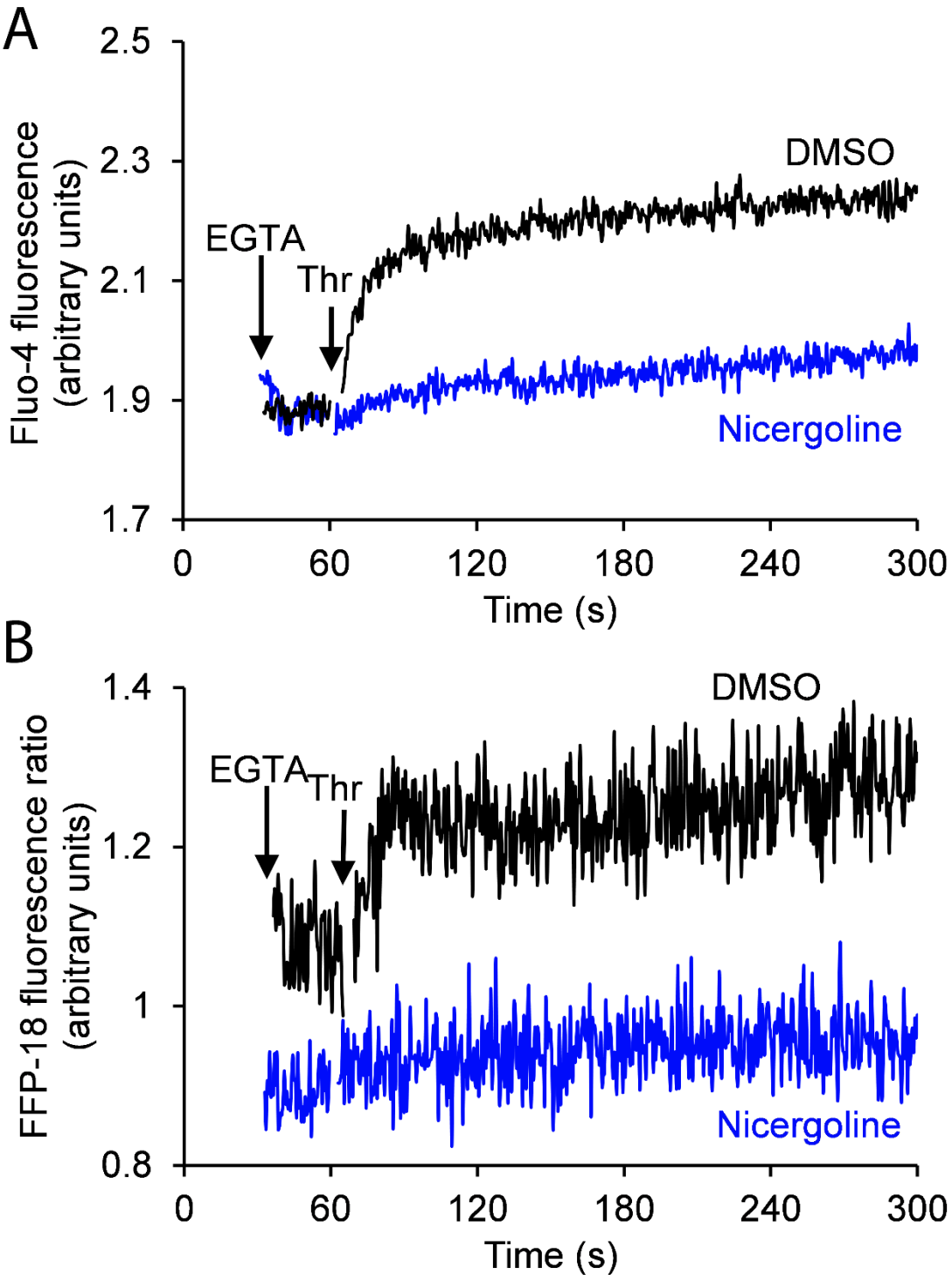

Figure 5. Nicergoline inhibits thrombin-evoked Ca^{2+} removal and pericellular Ca^{2+} accumulation in human platelets (A,B) Washed platelets suspended in supplemented HBS containing 2.5 µM Fluo-4 K^+ salt (A) or FFP-18-loaded platelets (B) were pre-treated with either DMSO or 100 µM nicergoline for 5 min at 37°C in the presence of continuous magnetic stirring. 1 mM EGTA was then added before the cells were stimulated with 0.5 $U.mL^{-1}$ thrombin. The results presented are representative of 5 and 6 experiments respectively

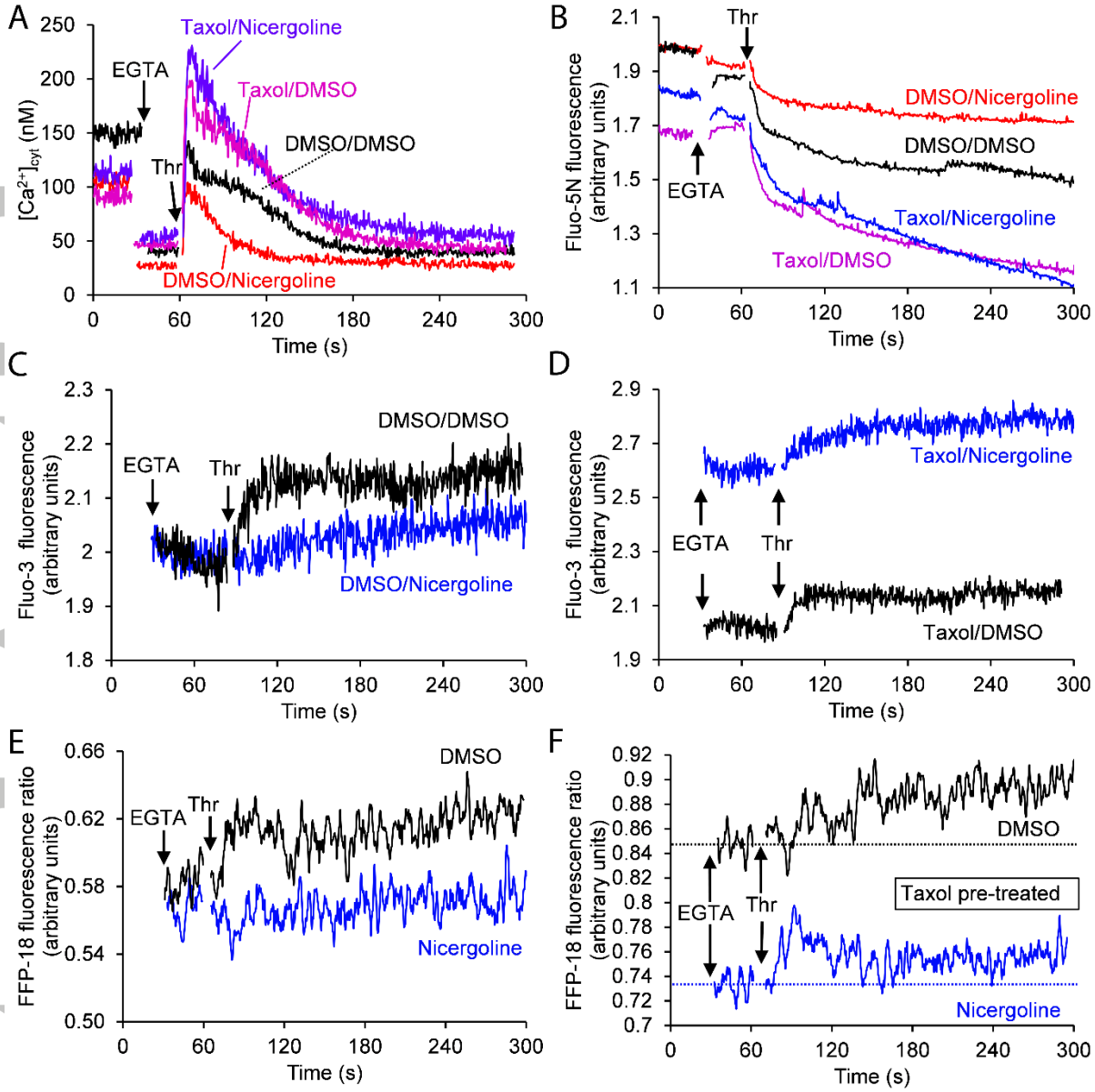

Figure 6. Stabilisation of platelet microtubules by prior treatment with taxol prevents nicergoline-induced disruption of thrombin-evoked Ca^{2+} signalling. Fura-2- (A), Fluo-5N-(B) or FFP-18- (E,F) loaded human platelets, or platelets suspended in supplemented HBS with 2.5 μM Fluo-3 K^+ salt (C,D) were pre-treated with either 100 μM taxol (A,B,D,F) or its vehicle, DMSO (A,B,C,E), for 30 minutes, followed by a further 5 minute incubation with either 100 μM nicergoline or its vehicle, DMSO. Platelets were subject to continuously magnetic stirring and held at 37°C throughout. EGTA (1 mM) was added before the cells were stimulated with 0.5 $U.mL^{-1}$ thrombin.

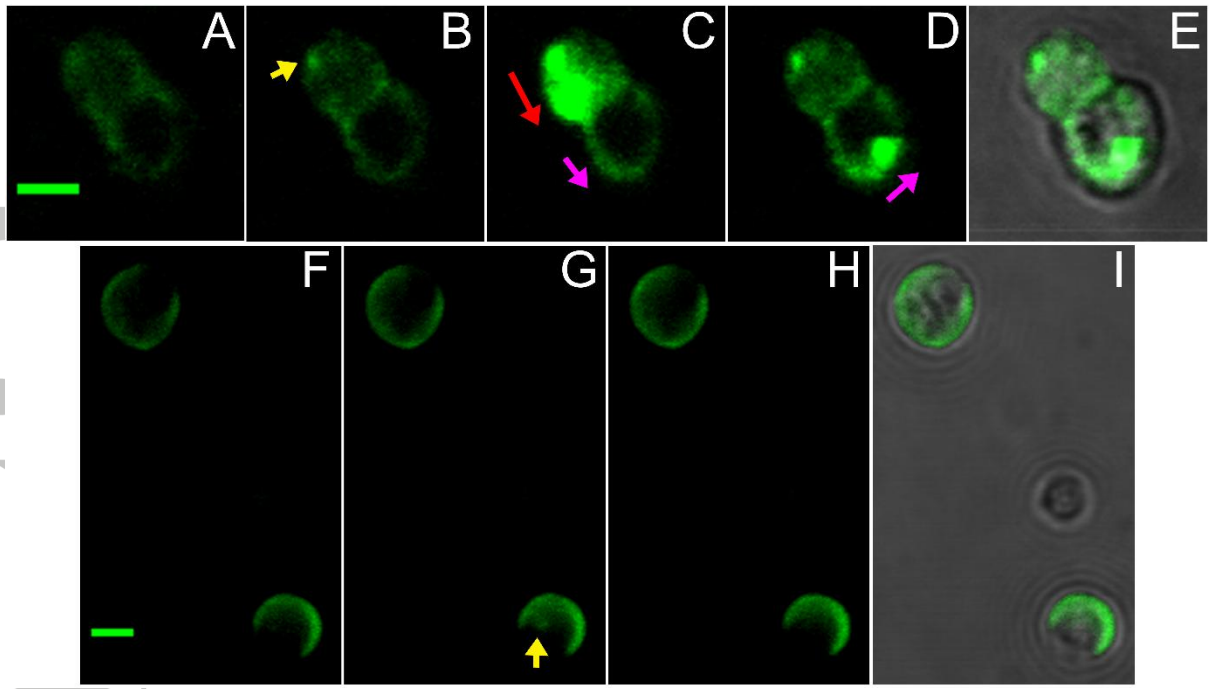

Figure 7 - Nicergoline treatment causes a dispersion of the pericellular Ca^{2+} hotspot, and inhibits the spread of the pericellular Ca^{2+} signal across the platelet. Cells were pretreated with either DMSO (A-E) or 100 μM nicergoline (F-I) for 5 min at 37°C in the presence of continuous magnetic stirring. The platelets were then added to a poly-L-lysine-coated chambered slide, and allowed to settle for 3 minutes. Excess platelet suspension was removed and the slides were washed twice with Ca^{2+}-free HBS containing 1 mM EGTA and 2.5 μM Fluo-4 K^+ salt, and platelets were then stimulated by addition of 0.5 $U.mL^{-1}$ thrombin. Fluorescence was then monitored using an Olympus Fluoview FV1200 confocal microscope at 0.5Hz for 5 minutes. Scale bar indicates 2 μm. Images shown at selected points during the recording period after thrombin addition (A and F – 0s; B – 52.8s; C – 162.8s; D and E – 224.4s; G – 70.4s ; H and I – 222.2s). Images show either Fluo-4 fluorescence alone (A-D; F-H) or overlaid with the transmitted light image (E,I). (A-E) DMSO-treated cells demonstrate a pericellular hotspot (yellow arrow; panel B), which then spreads across the cell (Panel C for top cell; Panels C and D for bottom cell). Note the reappearance of the pericellular hotspot in the same location it was initially seen in the top cell in panel D, in line with our previous findings. (F-I) Nicergoline-treated cells show an increased fluorescence over time from a more-dispersed cortical hotspot. As can be seen in Panel G, Nicergoline-treated cells show no (top cell) or weak spreading of Ca^{2+} (bottom cell; yellow arrow) in the pericellular region, which rarely crosses to the other side of the cell.

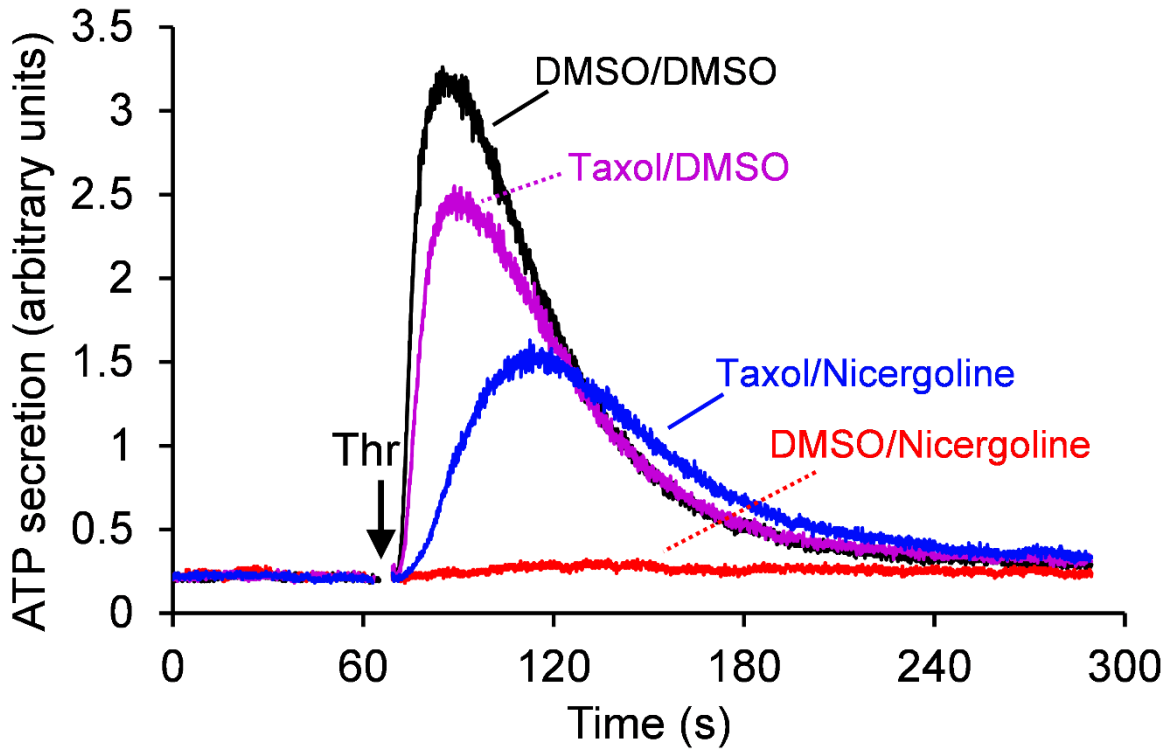

Figure 8. Pretreatment with taxol partially reverses the inhibitory effect of nicergoline on thrombin-evoked dense granule secretion. Washed platelet suspensions containing 1% [v/v] luciferin-luciferase were pre-treated with either 100 μM taxol or its vehicle, DMSO, for 30 minutes, followed by a further 5 minute incubation with either 100 μM nicergoline or its vehicle, DMSO. Platelets were subjected to continuous magnetic stirring and held at 37°C throughout. 1 mM EGTA was added immediately prior to the start of the experiment, and platelets were subsequently stimulated with 0.5 $U.mL^{-1}$ thrombin. The results presented are representative of 6 experiments.

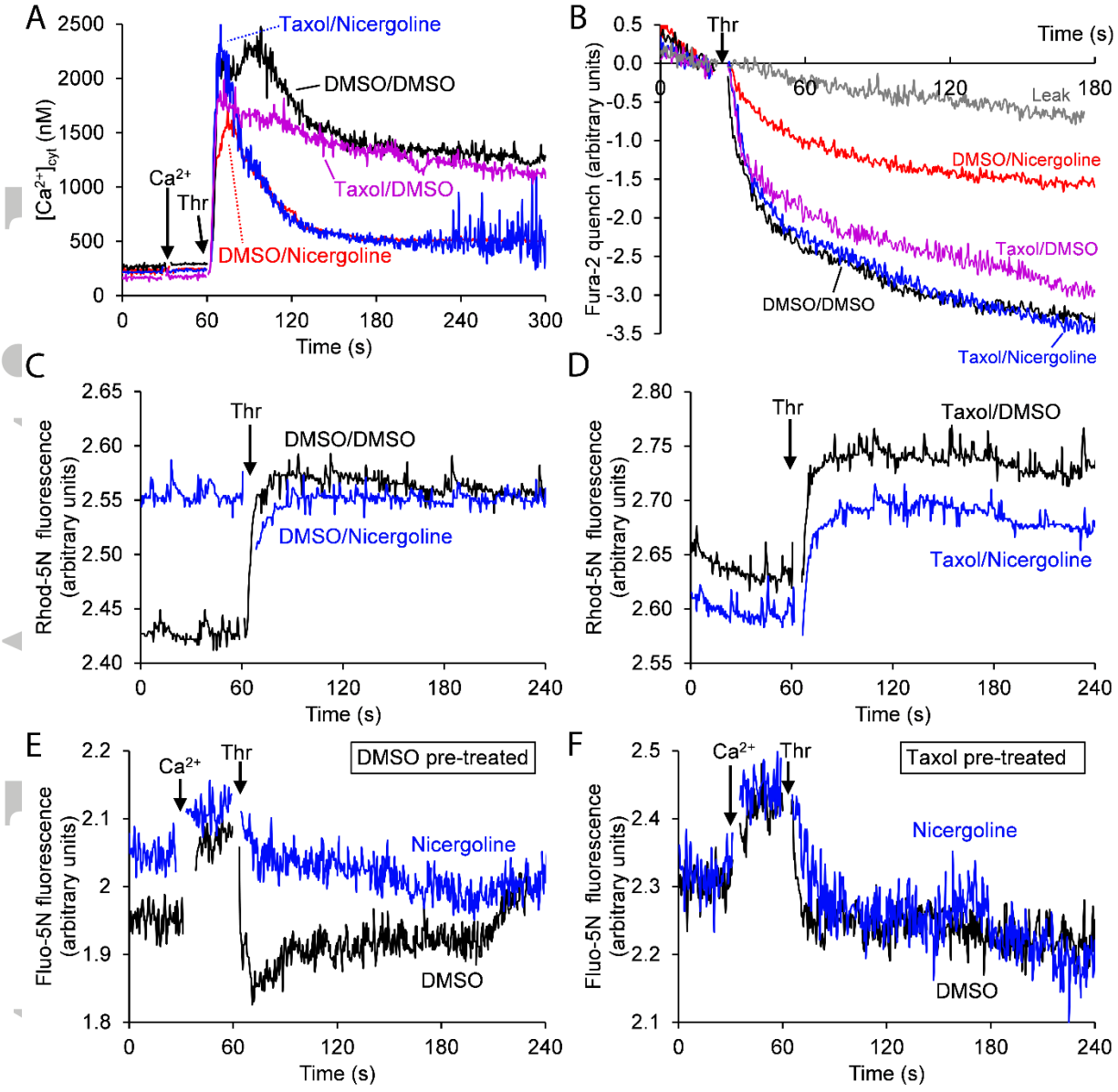

Figure 9. Pretreatment with taxol partially reverses the inhibitory effect of nicergoline on thrombin-evoked Ca^{2+} signalling elicited when platelets are stimulated in the presence of extracellular Ca^{2+}. (A,E,F) Fura-2-(A) or Fluo-5N-(E,F) loaded human platelets were pre-treated with either 100 μM taxol (A,F) or its vehicle, DMSO (A,F), for 30 minutes, followed by a further 5 minute incubation with either 100 μM nicergoline or its vehicle, DMSO. Platelets were subjected to continuous magnetic stirring and held at 37°C throughout. The extracellular Ca^{2+} concentration was raised to 1 mM by addition of 800 μM $CaCl_2$ before platelets were stimulated with 0.5 $U.ml^{-1}$ thrombin. (B) Fura-2-loaded platelets suspended in Ca^{2+}-free HBS supplemented with 0.1 $U.mL^{-1}$ apyrase were preincubated with either 100 μM taxol or its vehicle, DMSO, for 30 minutes, followed by a further 5 minute incubation with either 100 μM nicergoline or its vehicle, DMSO. Platelets were subjected to continuous magnetic stirring and held at 37°C throughout. Extracellular Ca^{2+} was chelated by addition of 500 μM EGTA, followed 30 seconds later by 1 mM $MnCl_2$. Platelets were stimulated 30 s later with 0.5 U mL^{-1} thrombin. (C,D) Washed platelets suspended in a supplemented HBS containing 300 μM $CaCl_2$ and 5 μM Rhod-5N K^+ salt were pre-treated with either 100 μM taxol (D) or its vehicle, DMSO (D), for 30 minutes, followed by a further 5 minutes incubation with either 100 μM nicergoline or its vehicle, DMSO. Platelets were subjected to continuous magnetic stirring and held at 37°C throughout. Platelets were subsequently stimulated by addition of 0.5 $U.mL^{-1}$ thrombin. The results presented are representative of 6-13 experiments.

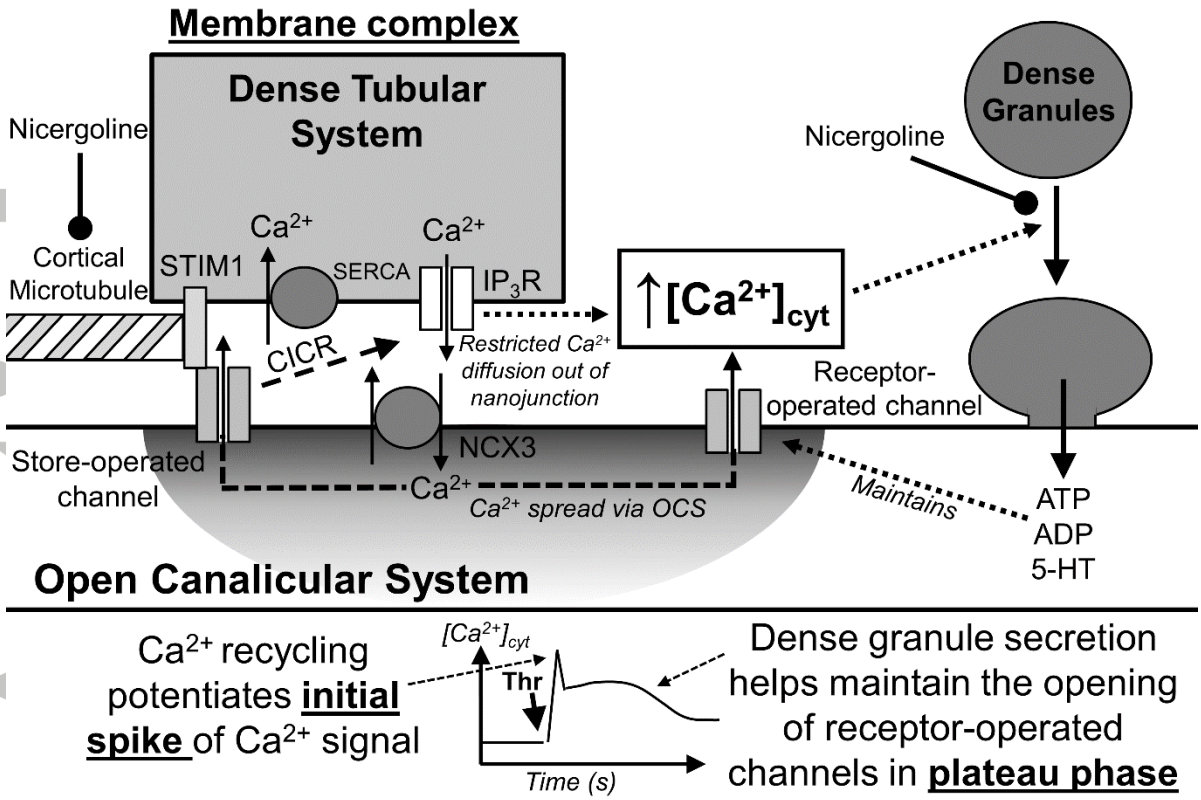

Figure 10. Proposed model for the role of the membrane complex in thrombin-evoked Ca^{2+} signalling, and its disruption by nicergoline. (A) We propose that the membrane complex is held together by the cortical microtubule bundle, which helps hold the DTS in close apposition to the OCS. One possible mechanism that may facilitate this interaction of the microtubules with the DTS, is the known ability of STIM1 to interact with microtubules via an EB1-containing complex (Grigoriev *et al*., 2008). The membrane complex helps potentiate the initial phase of Ca^{2+} entry by helping to transporting Ca^{2+} out of the cell via the NCX in large quantities (Sage *et al*., 2013), allowing it to accumulate at high concentrations in the OCS (Figure 7). This Ca^{2+} can recycle back into the cell contributing to the rise in $[Ca^{2+}]_{cyt}$ directly, as well as indirectly by facilitating store unloading via Ca^{2+}-induced Ca^{2+} release (CICR; Sage *et al.*, 2011; Sage *et al*., 2013; Figure 9E,F), and the activation of the store-operated channels via STIM1-dependent activation of an Orai1-containing ion channel (Braun *et al*., 2008; figure 7B). Upon nicergoline-treatment, the DTS stays attached to the disorganised microtubule bundle (Le Menn *et al*., 1979) leading to its redistribution around the cell (Figure 3) and dissociation of the membrane complex disperses the Ca^{2+} removal over a larger area of the OCS. This prevents Ca^{2+} accumulation within a small subregion of the OCS and thus reduces the pericellular Ca^{2+} concentration, preventing its ability to recycle back into the cell where it can both directly and indirectly affect the initial phase of the Ca^{2+} signal (Sage *et al*., 2013; Figure 9B,E,F). The reinstatement of Ca^{2+} recycling by taxol treatment is able to reinstate some of the Ca^{2+} signal and thus trigger a partial reversal of the effect of nicergoline on dense granule secretion. Ca^{2+} levels remain high due to the role of maintained Ca^{2+} entry through receptor-operator channels brought about by dense granule secretion, as previously demonstrated by studying platelets from patients with storage pool disorders (Lages and Weiss, 1999). Nicergoline has a taxol-insensitive effect on this phase of the Ca^{2+} signal by an additional effect on dense granule secretion and/or the signalling pathways triggered by ATP, ADP or 5-HT.

References

Behnke O (1967). Electron microscopic observations on the membrane systems of the rat blood platelet. *Anat Rec* **158**:121-138.

Blaustein MP, Lederer WJ (1999). Sodium/Calcium Exchange: Its Physiological Implications. *Physiol Rev* **79**: 763-854.

Braun A, Varga-Szabo D, Kleinschnitz C, Pleines I, Bender M, Austinat M *et al*., (2008). Orai1 (CRACM1) is the platelet SOC channel and essential for pathological thrombus formation. *Blood* **113***:* 2056–2063.

Canizares C, Vivar N, Grijalva J (1990). Thrombocytopathy due to a defect of the platelet membrane complex. *Acta Haematol* **83**: 99-104.

Cerecedo D, Cisneros B, Mondragon R, Gonzalez S, Galvan IJ (2010). Actin filaments and microtubule dual-granule transport in human adhered platelets: the role of alpha-dystrobrevins. *Br J Haematol* **149**: 124-136.

Diagouraga B, Grichine A, Fertin A, Wang J, Khochbin S, Sadoul K (2013). Motor-driven marginal band coiling promotes cell shape change during platelet activation. *J Cell Biol* **204**: 177-185.

Green D, Ts'ao CH, Cohen I, Rossi EC (1981). Haemorrhagic Thrombocytopathy Associated with Dilatation of the Platelet—Membrane Complex. *Br J Haematol* 1981; **48**: 595–600.

Grigoriev I, Gouveia SM, van der Vaart B, Demmers J, Smyth JT, Honnappa S *et al*., (2008). STIM1 is a MT-plus-end-tracking protein involved in remodelling of the ER. *Curr Biol* **18**: 177-182.

Harper AGS, Mason MJ, Sage SO (2009). A key role for dense granule secretion in potentiation of the Ca^{2+} signal arising from store-operated calcium entry in human platelets. *Cell Calcium* **45**: 413-420.

Harper AGS, Sage SO (2007). A key role for reverse Na^{+}/Ca^{2+} exchange influenced by the actin cytoskeleton in store-operated Ca^{2+} entry in human platelets: evidence against the de novo conformational coupling hypothesis. *Cell Calcium* **42**: 606-617.

Heemskerk JWM, Mattheij NJA, Cosemans JMEM (2013). Platelet-based coagulation: different populations, different functions. *J Thromb Haemost* **11**: 2-11.

Italiano Jr JE, Bergmeier W, Timari S, Falet H, Hartwig JH, Hoffmeister KM *et al*., (2003). Mechanisms and implications of platelets discoid shape. *Blood* **101**: 4789-4796.

Lages B, Weiss HJ (1999). Secreted dense granule adenine nucleotides promote calcium influx and the maintenance of elevated cytosolic calcium levels in stimulated human platelets. *Thromb Haemost* **81:** 286-292.

Lanza F, Cazenave JP, Beretz A, Sutter-Bay A, Kretz JG, Kieny R (1986). Potentiation by adrenaline of human platelet activation and the inhibition by the alpha-adrenergic antagonist nicergoline of platelet adhesion, secretion and aggregation. *Agents Actions* **18**; 586-595.

Le Menn R, Migne J, Probst-Djovakovich RJ (1979). Ultrastructural study on the effect of an inhibition of platelet aggregation. *Arzneimittelforschung* **29**: 1278-1282.

Meiamed I, Djaldetti M, Joshua H, Seligsohn U (1984). Association of the Hemophilia A Carrier State and Hemorrhagic Thrombocytopathy with Dilatation of the Platelet Membrane Complex. *Acta Haematol* **71**:381–387.

Parker RI, Bray GL, McKeown LP, White JG (1993). Failure to mobilize intracellular calcium in response to thrombin in a patient with familial thrombocytopathy characterized by macrothrombocytopenia and abnormal platelet membrane complexes. *J Lab Clin Med* **122**: 441-449.

Redondo PC, Harper AGS, Sage SO, Rosado JA (2007). Dual role of tubulin-cytoskeleton in store-operated calcium entry in human platelets. *Cell Signal* **19**: 2147-2154.

Rink TJ, Sage SO (1990). Calcium signalling in human platelets. *Ann Rev Physiol* **52**: 429-447.

Sadoul K, Wang J, Diagouraga B, Vitte AL, Buchou T, Rossini T *et al.*, (2012). HDAC6 controls the kinetics of platelet activation. *Blood* **120**:4215-4218.

Schwer HD, Lecine P, Tiwari S, Italiano JE, Hartwig JH, Shivdasani RA (2001). A lineage-restricted and divergent beta-tubulin isoform is essential for the biogenesis, structure and function of blood platelets. *Curr Biol* **11**: 579-586.

Sage SO, Pugh N, Farndale RW, Harper AGS (2013). Pericellular Ca^{2+} recycling potentiates thrombin-evoked Ca^{2+} signals in human platelets. *Physiol Rep* **1**:e00085.

Sage SO, Pugh N, Mason MJ, Harper AGS (2011). Monitoring the intracellular store Ca^{2+} concentration in agonist-stimulated, intact human platelets by using Fluo-5N. *J Thromb Haemost* **9**: 540–551.

Van Breemen C, Fameli N, Evans AM (2013). Pan-junctional sarcoplasmic reticulum in vascular smooth muscle: nanospace Ca^{2+} transport for site- and function-specific Ca^{2+} signalling. *J Physiol* **591**: 2043–2054.

van Nispen tot Pannerden HE, van Dijk SM, Du V, Heijnen HFG (2009). Platelet protein disulfide isomerase is localized in the dense tubular system and does not become surface expressed after activation. *Blood* **114**: 4738-4740.

van Nispen tot Pannerden H, de Haas F, Geerts W, Posthuma G, van Dijk S , Heijnen HFG (2010). The platelet interior revisited: electron tomography reveals tubular α-granule subtypes. *Blood* **116**: 1147-1156.

White JG (1968). Effects of colchicine and vinca alkaloids on human platelets. II. Changes in the dense tubular system and formation of an unusual inclusion in incubated cells. *Am J Pathol* **53**:447-461.

White JG (1972). Interaction of membrane systems in blood platelets. *Am J Pathol* **66**: 295-312.